Novel effects of size disorder on the electronic and magnetic properties of rare earth manganates of the type $La_{0.7-x}Ln_xBa_{0.3}MnO_3$ (Ln = Pr, Nd, Gd or Dy) with large average radius of the A-site cations

Asish K Kundu[1], Md Motin Seikh[1,2], K Ramesha[3] and C N R Rao[1,2,4]

[1] Chemistry and Physics of Materials Unit, Jawaharlal Nehru Centre for Advanced Scientific Research, Jakkur PO, Bangalore-560 064, India
[2] Solid State and Structural Chemistry Unit, Indian Institute of Science, Bangalore-560 012, India
[3] Materials Department, University of California, Santa Barbara, CA 93106, USA

E-mail: cnrrao@jncasr.ac.in

Abstract

The electronic and magnetic properties of four series of rare earth manganates of the general formula $La_{0.7-x}Ln_xBa_{0.3}MnO_3$ (Ln = Pr, Nd, Gd or Dy) have been investigated to examine the effect of large size disorder in a system where the average radius of the A-site cations, $\langle r_A \rangle$, remains high (1.216–1.292 Å) and the Mn^{3+}/Mn^{4+} ratio is kept constant. The size disorder, as measured by the Attfield σ^2 parameter, has been varied over a wide range of 0.001 and 0.03 $Å^2$. As x is increased, the materials exhibit a decrease in the ferromagnetic Curie temperature, T_c, or lose ferromagnetism entirely. This is accompanied by an insulator–metal (I–M) transition, with T_{IM} decreasing with increasing x, or an entirely insulating behaviour. The insulating behaviour and loss of ferromagnetism occurs when σ^2 is close to 0.02 $Å^2$. Thus, in the Ln = Nd, Gd and Dy series, the non-magnetic insulating behaviour occurs at x values of 0.7, 0.5 and 0.3 respectively. Where an I–M transition occurs, $T_{IM} < T_c$, indicating the presence of a ferromagnetic insulating regime. The absence of long-range ferromagnetism in some of the compositions is accompanied by a divergence between the zero-field-cooled and the field-cooled magnetization data. The ferromagnetic or non-magnetic insulating state is due to phase separation wherein ferromagnetic clusters are present in an insulating matrix. The non-magnetic insulating compositions can be rendered ferromagnetic and metallic by decreasing σ^2 while keeping $\langle r_A \rangle$ constant. This extraordinary display of the effect of size disorder on the properties of the rare earth manganates is noteworthy.

[4] Author to whom any correspondence should be addressed.

1. Introduction

Rare-earth manganates of the type $Ln_{1-x}A_xMnO_3$ (Ln = rare earth, A = alkaline earth) exhibit many interesting properties such as colossal magnetoresistance, charge ordering, orbital ordering and electronic phase separation [1–5]. All these properties are highly sensitive to the average radius of the A-site cation, $\langle r_A \rangle$, as well as the size disorder arising from the mismatch between the A-site cations [4, 6, 7]. A detailed study of several compositions of the $La_{0.7-x}Ln_xCa_{0.3}MnO_3$ series of manganates has shown the occurrence of electronic phase separation above a critical composition x_c [8–10]. In this series of manganates, $\langle r_A \rangle$ decreases markedly with increase in x, accompanied by an increase in size disorder. Above x_c, the materials become insulating and do not show ferromagnetism, the x_c values corresponding to the critical $\langle r_A \rangle$ value, $\langle r_A^c \rangle$, of 1.18 Å. Electronic phase separation occurs in the region of $\langle r_A^c \rangle$ [8–10]. In order to fully appreciate the effect of the size mismatch between A-site cations, we considered it important to investigate a series of manganates, where the $\langle r_A \rangle$ remains substantially large, well above $\langle r_A^c \rangle$ through the series, but the size disorder increases significantly. $La_{0.7}Ba_{0.3}MnO_3$, with $\langle r_A \rangle$ of 1.292 Å, is a good ferromagnetic metal with a ferromagnetic transition temperature, T_c, of 340 K [11]. The T_c is, however, lower than the value expected on the basis of the large A-site cation radius, because of the mismatch between the A-site cations [7, 12, 13]. Thus, the size variance, σ^2, defined as $\sigma^2 = \sum x_i r_i^2 - \langle r_A \rangle^2$, where x_i is the fractional occupancy of A-site ions, r_i is the corresponding ionic radius [12], is quite large, the value being 0.014 Å^2. $Pr_{0.7}Ba_{0.3}MnO_3$ [14, 15], with a $\langle r_A \rangle$ of 1.266 Å and σ^2 of 0.018 Å^2, shows a distinct ferromagnetic transition around 190 K due to long-range ferromagnetic ordering and an insulator–metal (I–M) transition at a lower temperature. The properties of $Nd_{0.7}Ba_{0.3}MnO_3$ with an $\langle r_A \rangle$ of 1.255 Å and σ^2 of 0.020 Å^2, however, appear to be quite different, with an unusual insulating behaviour [16]. We have investigated the effect of substitution of La in $La_{0.7}Ba_{0.3}MnO_3$ by the smaller rare earth ions Pr, Nd, Gd and Dy, on the magnetic and electron transport properties, to understand the evolution of the insulating behaviour accompanying the disappearance of ferromagnetism, primarily arising from size disorder. It is to be noted that, in a given series of manganates, the size disorder increases considerably with x, although $\langle r_A \rangle$ remains in the range 1.216–1.292 Å, and the carrier concentration or the Mn^{3+}/Mn^{4+} ratio is constant. In order to evaluate the effect of size disorder quantitatively, we have varied σ^2 in two series of manganates of the type $Ln_{0.7-x}Ln'_xA_{0.3-y}A'_yMnO_3$, wherein $\langle r_A \rangle$ is kept constant at 1.266 and 1.216 Å, corresponding to the $\langle r_A \rangle$ of $Pr_{0.7}Ba_{0.3}MnO_3$ and $Gd_{0.7}Ba_{0.3}MnO_3$ respectively.

2. Experimental procedure

Polycrystalline samples of $La_{0.7-x}Ln_xBa_{0.3}MnO_3$ (Ln = Pr, Nd, Gd and Dy) were prepared by the ceramic method. Stoichiometric mixtures of the respective rare earth oxides, alkaline earth carbonates and MnO_2 were weighed in the desired proportions and milled for a few hours with propanol. The mixtures were dried, and calcined in air at 950 °C, followed by heating at 1000 and 1100 °C for 12 h each in air. The powders thus obtained were pelletized and the pellets sintered at 1400 °C for 24 h in air. Two series of manganates of the general formula $Ln_{0.7-x}Ln'_xA_{0.3-y}A'_yMnO_3$, with fixed $\langle r_A \rangle$ values of 1.266 and 1.216 Å, were prepared by the same method. Composition analysis was carried out using energy dispersive x-ray analysis (EDAX) using a LEICA S440I scanning electron microscope fitted with a Si–Li detector. The oxygen stoichiometry was determined by iodometric titrations. The error in oxygen content was ±0.02. The oxygen stoichiometry in the $La_{0.7-x}Ln_xBa_{0.3}MnO_3$ and $Ln_{0.7-x}Ln'_xA_{0.3-y}A'_yMnO_3$ series studied by us was generally 2.97 ± 0.03.

Table 1. Crystal structure and properties of $La_{0.7-x}Ln_xBa_{0.3}MnO_3$ (Ln = Pr, Nd, Gd or Dy).

Composition	$\langle r_A \rangle$ (Å)	σ^2 (Å^2)	Space group	Lattice parameters (Å)[a] a	b	$c/\sqrt{2}$	T_c (K)	T_{IM} (K)
$x = 0.0$	1.292	0.014	*Pnma*	5.534	5.529	5.529	340	—
			Ln = Pr					
$x = 0.1$	1.289	0.014	*Pnma*	5.529	5.514	5.527	320	—
$x = 0.3$	1.281	0.016	*Pnma*	5.527	5.523	5.519	285	270
$x = 0.5$	1.274	0.017	*Pnma*	5.517	5.510	5.503	235	210
$x = 0.6$	1.270	0.017	*Pnma*	5.520	5.500	5.507	210	175
$x = 0.7$	1.266	0.018	*Pnma*	5.512	5.495	5.505	190	150
			Ln = Nd					
$x = 0.3$	1.276	0.017	*Pnma*	5.511	5.513	5.524	250	240
$x = 0.5$	1.266	0.018	*Pnma*	5.507	5.506	5.507	190	160
$x = 0.7$	1.255	0.020	*Pnma*	5.498	5.497	5.498	150	—
			Ln = Gd					
$x = 0.1$	1.281	0.016	*Pnma*	5.527	5.524	5.525	280	275
$x = 0.2$	1.270	0.019	*Pnma*	5.527	5.516	5.517	210	190
$x = 0.3$	1.259	0.021	*Pnma*	5.521	5.511	5.511	150	120
$x = 0.5$	1.238	0.025	*Pnma*	5.496	5.491	5.497	—	—
$x = 0.6$	1.227	0.026	*Pnma*	5.496	5.487	5.488	—	—
$x = 0.7$	1.216	0.027	*Pnma*	5.479	5.471	5.477	—	—
			Ln = Dy					
$x = 0.1$	1.279	0.017	*Pnma*	5.530	5.515	5.525	270	270
$x = 0.2$	1.266	0.020	*Pnma*	5.521	5.508	5.511	190	170
$x = 0.3$	1.252	0.023	*Pnma*	5.510	5.501	5.497	—	—
$x = 0.4$	1.239	0.026	*Pnma*	5.507	5.496	5.496	—	—

[a] Uncertainty is approximately ±0.004.

The phase purity of the manganates was established by recording the x-ray diffraction patterns in the 2θ range 10°–80° with a Seiferts 3000 TT diffractometer using Cu Kα radiation. Electrical resistivity (ρ) measurements were carried out from 320 to 20 K by the four-probe method. Magnetization (M) measurements were made with a vibrating sample magnetometer (VSM) (Lakeshore 7300) and with a Quantum Design MPMS 5XL magnetometer. In the VSM and MPMS 5XL measurements the data were collected in the 300–50 and 350–10 K ranges, respectively. The temperature dependence of the zero-field-cooled (ZFC), field-cooled (FC) and the frequency dependence AC susceptibility measurements were recorded in the MPMS 5XL magnetometer. For the ZFC measurement the sample was cooled down from 350 to 10 K in zero-field, and for the FC measurement the sample was cooled to 10 K in an applied field of 500 Oe. The data were all recorded during reheating the sample.

3. Results and discussion

All the manganate compositions of the formula $La_{0.7-x}Ln_xBa_{0.3}MnO_3$ (Ln = Pr, Nd, Gd and Dy) could be indexed on an orthorhombic structure with the *Pnma* space group. We have listed the lattice parameters of the various compositions in table 1 along with the values of $\langle r_A \rangle$ and the size variance σ^2. The lattice parameters as well as the volume of the unit cell

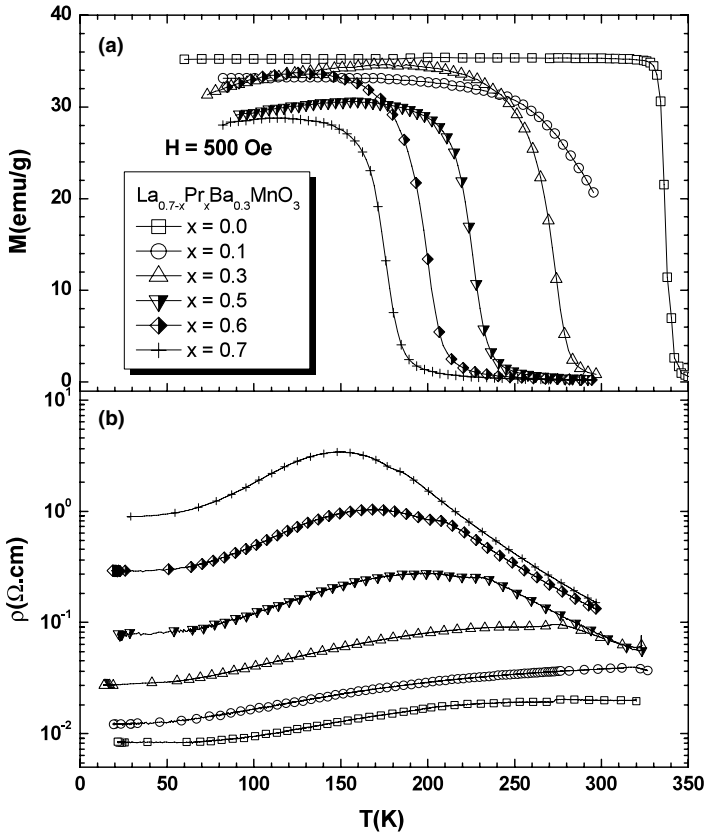

Figure 1. Temperature variation of (a) the magnetization, M, ($H = 500$ Oe) and (b) the electrical resistivity, ρ, of $La_{0.7-x}Pr_xBa_{0.3}MnO_3$.

vary linearly with $\langle r_A \rangle$, as expected. In figure 1, we show the magnetization and resistivity data of the $La_{0.7-x}Pr_xBa_{0.3}MnO_3$ series of manganates. The T_c value decreases progressively with increasing x, reaching a value of 190 K in $Pr_{0.7}Ba_{0.3}MnO_3$. The value of the saturation magnetization decreases only slightly with the increase in x (35–29 emu g^{-1} at 60 K in the $x = 0.0$–0.7 range). The material is metallic at room temperature up to $x = 0.3$ and exhibits a broad I–M transition when $x \geqslant 0.3$, the transition temperature, T_{IM}, decreasing with increasing x. $Pr_{0.7}Ba_{0.3}MnO_3$ itself shows an I–M transition around 150 K (T_{IM}) which is lower than the T_c value. This value of T_{IM} is somewhat higher than that reported by Heilman *et al* [14]. It is interesting that, as x approaches 0.7, the difference between T_c and T_{IM} increases, with the latter becoming considerably lower than T_c. $Pr_{0.7}Ba_{0.3}MnO_3$ is, therefore, a ferromagnetic insulator in the regime between T_c and T_{IM} (190–150 K).

The magnetization and resistivity data of $La_{0.7-x}Nd_xBa_{0.3}MnO_3$ are shown in figure 2. Here again, the T_c value decreases with increasing x, and there is a marked decrease in the value of the saturation magnetization as well. There is a sharp increase in magnetization with an apparent T_c of ∼150 K in $Nd_{0.7}Ba_{0.3}MnO_3$. But the saturation moment is small, suggesting there may be no long-range ferromagnetic ordering in the material. Thus, the saturation magnetization is 30 emu g^{-1} at $x = 0.3$ and $Nd_{0.7}Ba_{0.3}MnO_3$ ($x = 0.7$) does not exhibit clear saturation down to low temperatures. The highest value of magnetization obtained for $Nd_{0.7}Ba_{0.3}MnO_3$ is 18 emu g^{-1} at 60 K compared to 35 emu g^{-1} in $La_{0.7}Ba_{0.3}MnO_3$.

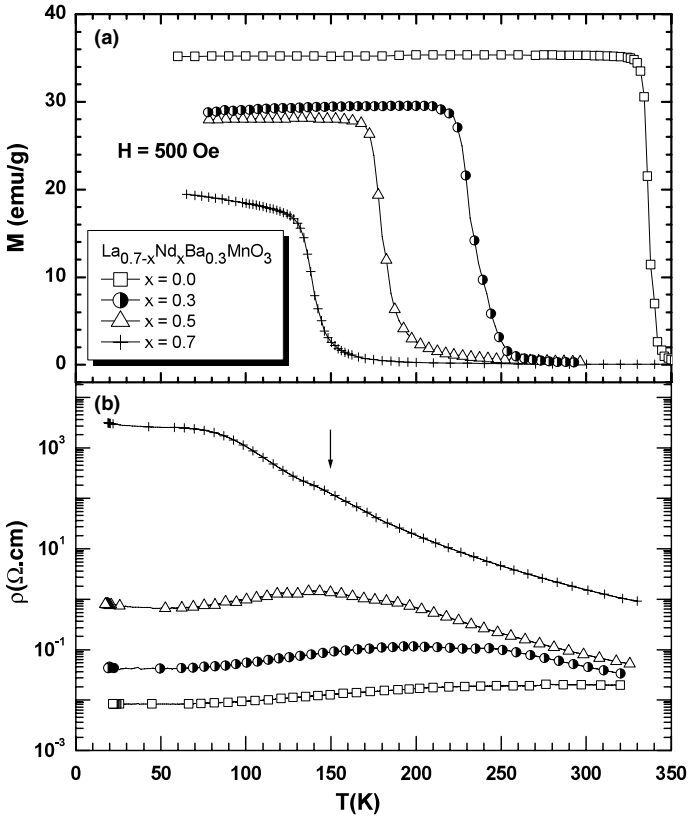

Figure 2. Temperature variation of (a) the magnetization, M, ($H = 500$ Oe) and (b) the electrical resistivity, ρ, of $La_{0.7-x}Nd_xBa_{0.3}MnO_3$. The arrow mark is explained in text.

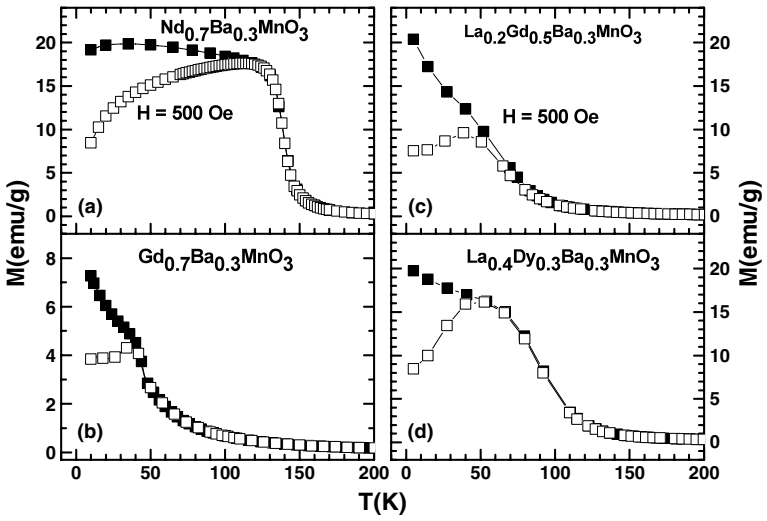

Figure 3. Temperature variation of the magnetization, M, of (a) $Nd_{0.7}Ba_{0.3}MnO_3$ (b) $Gd_{0.7}Ba_{0.3}MnO_3$ (c) $La_{0.2}Gd_{0.5}Ba_{0.3}MnO_3$ and (d) $La_{0.4}Dy_{0.3}Ba_{0.3}MnO_3$ (at $H = 500$ Oe). The solid symbols represent FC and open symbols represent ZFC data, respectively.

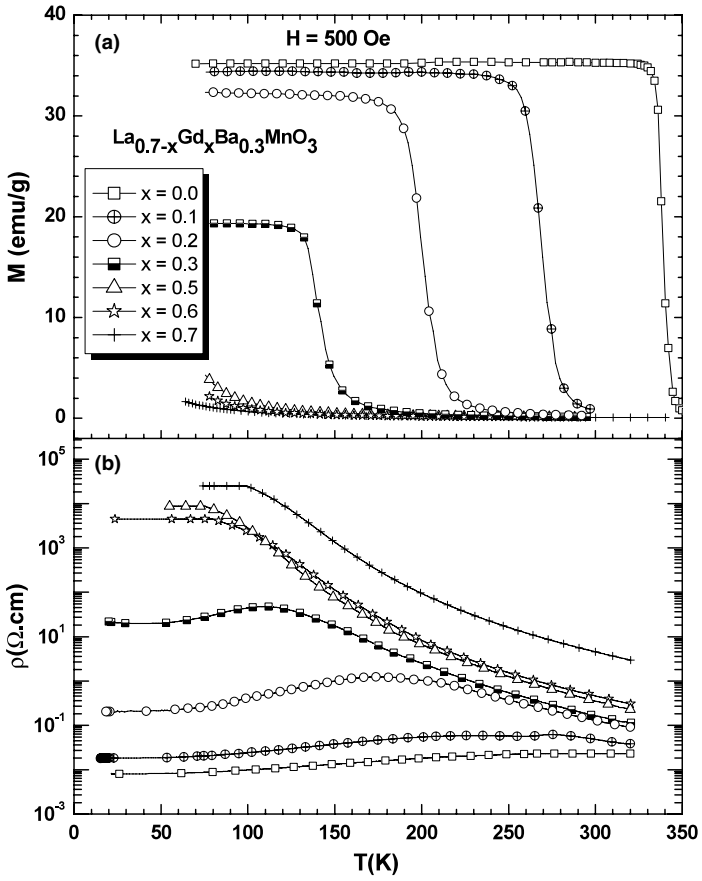

Figure 4. Temperature variation of (a) the magnetization, M, ($H = 500$ Oe) and (b) the electrical resistivity, ρ, of $La_{0.7-x}Gd_xBa_{0.3}MnO_3$.

The saturation magnetic moments in $Nd_{0.7}Ba_{0.3}MnO_3$ and $La_{0.7}Ba_{0.3}MnO_3$ are 0.8 and 1.5 μ_B respectively, while that in $Pr_{0.7}Ba_{0.3}MnO_3$ is 1.2 μ_B (at $H = 500$ Oe). Accordingly, the ZFC and FC data show considerable divergence below T_c (figure 3(a)), unlike in $Pr_{0.7}Ba_{0.3}MnO_3$. The resistivity behaviour of $La_{0.7-x}Nd_xBa_{0.3}MnO_3$ is quite different from that of $La_{0.7-x}Pr_xBa_{0.3}MnO_3$. The $La_{0.7-x}Nd_xBa_{0.3}MnO_3$ compositions show a broad I–M transition when $x = 0.3$ and 0.5, but the 0.7 composition is an insulator with high resistivity. The resistivity behaviour of $Nd_{0.7}Ba_{0.3}MnO_3$ found by us differs from the earlier report [16] to some extent. We do not find a distinct I–M transition in this material nor two resistivity peaks around T_{IM}. We barely see a shoulder around T_c as shown by the arrow in figure 2. Since $Nd_{0.7}Ba_{0.3}MnO_3$ does not show long-range ferromagnetic ordering, it would appear that the material contains ferromagnetic clusters in the insulating matrix. The double peaks in resistivity data reported earlier [16] or the shoulder near T_c found by us also suggest such phase separation. Ferromagnetic clusters in an insulating matrix would also be present in other compositions ($0.0 < x < 0.7$) where $T_c > T_{IM}$.

In the $La_{0.7-x}Gd_xBa_{0.3}MnO_3$ series, progressive substitution of La by Gd causes the ferromagnetic features to disappear entirely when $x \geqslant 0.5$ (figure 4(a)). Even when $x = 0.3$, the T_c is only 155 K and the saturation magnetization is 20 emu g^{-1} at 60 K.

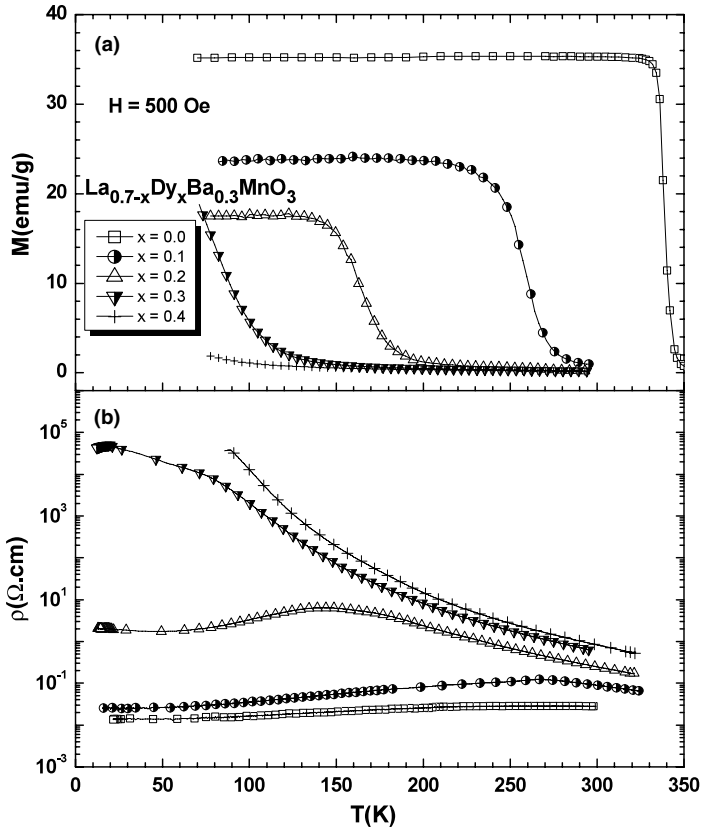

Figure 5. Temperature variation of (a) the magnetization, M, ($H = 500$ Oe) and (b) the electrical resistivity, ρ, of $La_{0.7-x}Dy_xBa_{0.3}MnO_3$.

The $x \geqslant 0.5$ compositions exhibit divergence between the ZFC and FC magnetization data (see figures 3(b) and (c)), indicating the absence of long-range ferromagnetic ordering. AC susceptibility measurements reveal a weakly frequency-dependent peak at 50 and 40 K respectively in the $x = 0.5$ and 0.7 compositions. These compositions also fail to show the I–M transitions in the resistivity data, whereas the samples with $x < 0.5$ show distinct I–M transitions. The compositions with $x > 0.5$ are insulating just as $Nd_{0.7}Ba_{0.3}MnO_3$ and the resistivity of $Gd_{0.7}Ba_{0.3}MnO_3$ is higher than that of $Nd_{0.7}Ba_{0.3}MnO_3$ (figure 4(b)). In the $La_{0.7-x}Dy_xBa_{0.3}MnO_3$ series, ferromagnetism does not occur for $x > 0.2$ (figure 5(a)). The $x = 0.2$ composition shows an apparent T_c of 180 K, but the saturation magnetization is very low (18 emu g^{-1}). The $x = 0.2$ composition shows the I–M transition, but all the compositions with $x > 0.2$ are insulating, the resistivity being higher than that of the corresponding Gd and Nd substituted manganates. The ZFC and FC data of the $x = 0.3$ composition show divergence (figure 3(d)), indicating the absence of long-range ferromagnetic ordering.

In both the $La_{0.7-x}Gd_xBa_{0.3}MnO_3$ and $La_{0.7-x}Dy_xBa_{0.3}MnO_3$ series of manganates, ferromagnetism disappears as x increases, accompanied by an insulating behaviour. The apparent ferromagnetic transitions with a low saturation magnetization observed for $x = 0.3$ and 0.2 at 150 and 180 K respectively in the Gd and Dy derivatives, and associated with T_{IM} values lower than T_c, pointing to the presence of a ferromagnetic insulating state. It is likely

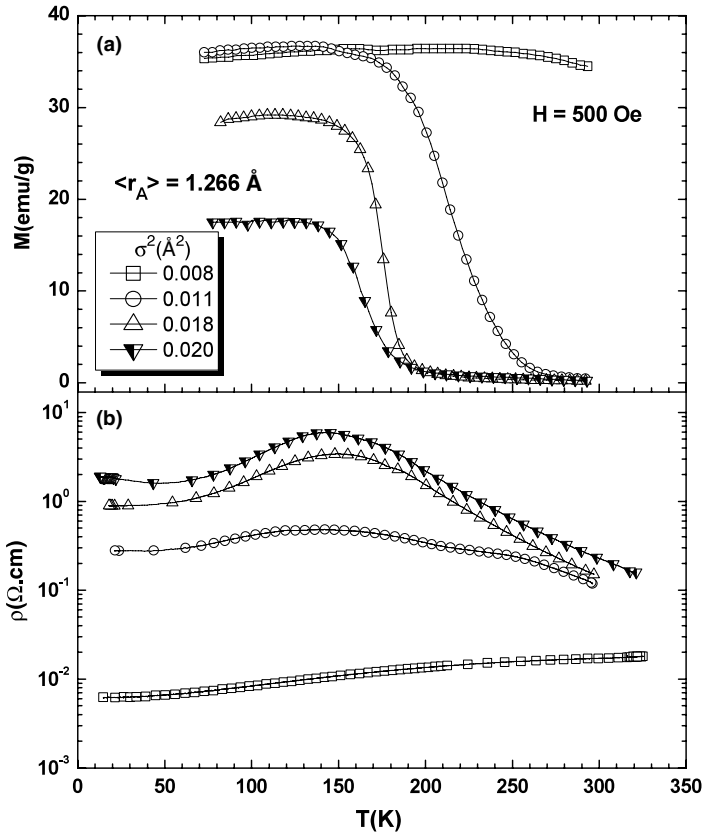

Figure 6. Temperature variation of (a) the magnetization, M, ($H = 500$ Oe) and (b) the electrical resistivity, ρ, of $Ln_{0.7-x}Ln'_xA_{0.3-y}A'_yMnO_3$ with a fixed $\langle r_A \rangle$ value of 1.266 Å.

that, in all the compositions where the ferromagnetic insulating state occurs, there is phase separation wherein ferromagnetic clusters are present in an insulating matrix. It is interesting that the difference between T_c and T_{IM} manifests itself only when σ^2 is considerably large. In the four series of $La_{0.7-x}Ln_xBa_{0.3}MnO_3$ studied by us, the difference between T_c and T_{IM} starts emerging when the $\sigma^2 = 0.016$ Å^2, although the $\langle r_A \rangle$ is relatively large, being around 1.28 Å. Clearly the size disorder plays a crucial role in determining the properties of these manganates.

In order to investigate the effect of size disorder quantitatively, we have examined the compositions with constant $\langle r_A \rangle$ values corresponding to $Pr_{0.7}Ba_{0.3}MnO_3$ and $Gd_{0.7}Ba_{0.3}MnO_3$ respectively, and varied the σ^2. In table 2, we list the structural parameters of two series of manganates. The magnetization and resistivity data of the compositions with $\langle r_A \rangle = 1.266$ Å are shown in figure 6. We see that T_c increases with decreasing σ^2 and the material becomes metallic at the lowest value of $\sigma^2 = 0.008$ Å^2, while I–M transitions occur in the σ^2 range 0.02–0.01 Å^2. This is indeed a nice result in that a system normally showing an I–M transition becomes metallic as the size disorder is decreased. The effect of size disorder is seen more vividly when the $\langle r_A \rangle$ value is 1.216 Å, corresponding to $Gd_{0.7}Ba_{0.3}MnO_3$, a non-magnetic insulating material. However, when the size disorder is decreased, the material becomes ferromagnetic, with T_c going up to ∼300 K at the lowest value of σ^2 (figure 7(a)). As σ^2 decreases, the insulating behaviour also gives way to metallic behaviour. The T_c

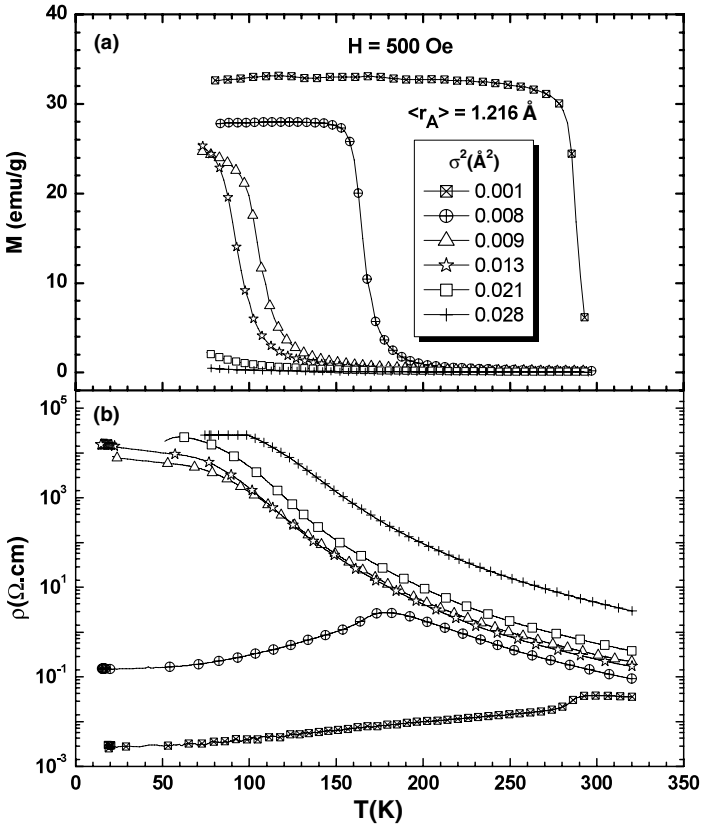

Figure 7. Temperature variation of (a) the magnetization, M, ($H = 500$ Oe) and (b) the electrical resistivity, ρ, of $Ln_{0.7-x}Ln'_xA_{0.3-y}A'_yMnO_3$ with a fixed $\langle r_A \rangle$ value of 1.216 Å.

Table 2. Crystal structure of $Ln_{0.7-x}Ln'_xA_{0.3-y}A'_yMnO_3$ with fixed $\langle r_A \rangle$.

Composition	σ^2 (Å^2)	Space group	Lattice parameters (Å) a	b	$c/\sqrt{2}$	V (Å^3)
		$\langle r_A \rangle = 1.266$ Å				
$La_{0.7}Ba_{0.14}Sr_{0.16}MnO_3$	0.008	*Pnma*	5.520	5.496	5.596	236
$La_{0.7}Ba_{0.21}Ca_{0.09}MnO_3$	0.011	*Pnma*	5.537	5.508	5.501	237
$Pr_{0.7}Ba_{0.3}MnO_3$	0.018	*Pnma*	5.512	5.495	5.505	236
$La_{0.5}Dy_{0.2}Ba_{0.3}MnO_3$	0.021	*Pnma*	5.521	5.508	5.511	237
		$\langle r_A \rangle = 1.216$ Å				
$La_{0.7}Sr_{0.08}Ca_{0.22}MnO_3$	0.001	*Pnma*	5.467	5.468	5.476	232
$Nd_{0.7}Ba_{0.06}Sr_{0.24}MnO_3$	0.008	*Pnma*	5.474	5.464	5.469	232
$Pr_{0.7}Ba_{0.125}Ca_{0.125}MnO_3$	0.009	*Pnma*	5.485	5.474	5.474	233
$Nd_{0.7}Ba_{0.165}Ca_{0.135}MnO_3$	0.013	*Pnma*	5.490	5.473	5.469	233
$Sm_{0.7}Ba_{0.24}Ca_{0.06}MnO_3$	0.021	*Pnma*	5.483	5.472	5.473	233
$Gd_{0.7}Ba_{0.3}MnO_3$	0.028	*Pnma*	5.479	5.471	5.477	233

values (in figures 6(a) and 7(a)) vary linearly with σ^2 with the slopes of $10\,235 \pm 2191$ and $17\,068 \pm 3260$ K Å^{-2} for $\langle r_A \rangle$ of 1.266 Å and $\langle r_A \rangle$ of 1.216 Å, respectively. The corresponding

values of intercepts, T_c^0, are 374 ± 5 and 305 ± 3 K, respectively. These values are comparable to those reported in the literature for other series of manganates [10, 17].

4. Conclusions

The present study on the electronic and magnetic properties of the four series of $La_{0.7-x}Ln_xBa_{0.3}MnO_3$ (Ln = Pr, Nd, Gd and Dy) manganates, wherein the average radius of the A-site cation generally remains large (1.216–1.292 Å), but the size disorder is also considerable, has revealed certain interesting aspects. Since the band narrowing due to small $\langle r_A \rangle$ is entirely avoided, the predominant effect is due to size disorder. It is interesting that these materials show a progressive decrease in the ferromagnetic T_C, eventually giving rise to a non-magnetic insulating behaviour. Accordingly, with increasing x or σ^2, the material exhibits a ferromagnetic insulating phase due to the presence of ferromagnetic clusters in the insulating matrix. At large x or σ^2, where some of the compositions lose ferromagnetism and become insulating, there is evidence for clusters with short-range ferromagnetic interaction. In the insulating regime caused by size disorder, there is clearly phase separation due to the presence of ferromagnetic clusters in an insulating matrix. The phase separation is minimized or eliminated by decreasing σ^2, as evidenced from the change of the non-magnetic insulating phase to a ferromagnetic metallic state.

Acknowledgments

The authors would like to thank BRNS (DAE), India, for support of this research. AKK thanks the University Grants Commission and MMS thanks CSIR, India, for a research fellowship award.

References

[1] Rao C N R and Raveau B (ed) 1998 *Colossal Magnetoresistance, Charge Ordering, and Related Properties of Manganese Oxides* (Singapore: World Scientific)
[2] Tokura Y (ed) 1999 *Colossal Magnetoresistance Oxides* (London: Gordon and Breach)
[3] Ramirez A P 1997 *J. Phys.: Condens. Matter* **9** 8171
[4] Rao C N R 2000 *J. Phys. Chem.* B **104** 5877
[5] Dagotto E (ed) 2003 *Nano Scale Phase Separation and Colossal Magnetoresistance* (Berlin: Sringer)
[6] Rao C N R and Vanitha P V 2002 *Curr. Opin. Solid State Mater. Sci.* **6** 97
[7] Rogriguez-Martinez L M and Attfield J P 2000 *Phys. Rev.* B **63** 024424
[8] Uehara M, Mori S, Chen C H and Cheong S W 1999 *Nature* **399** 560
[9] Balagurov A M, Pomjakushin V Yu, Sheptyakov D V, Aksenov V L, Fischer P, Keller L, Gorbenko O Yu, Kaul A R and Babushkina N A 2001 *Phys. Rev.* B **64** 024420
[10] Sudheendra L and Rao C N R 2003 *J. Phys.: Condens. Matter* **15** 3029 and references therein
[11] Ju H L, Gopalakrishnan J, Peng J L, Li Qi, Xiong G C, Venkatesan T and Greene R L 1995 *Phys. Rev.* B **51** 6143
[12] Rogriguez-Martinez L M and Attfield J P 1996 *Phys. Rev.* B **54** R15622
[13] Mahesh R, Mahendiran R, Raychaudhuri A K and Rao C N R 1995 *J. Solid State Chem.* **120** 204
[14] Heilman A K, Xue Y Y, Lorenz B, Campbell B J, Cmaidalka J, Meng R L, Yang Y S and Chu C W 2002 *Phys. Rev.* B **65** 214423
[15] Ellouze M, Boujelben W, Cheikhrouhou A, Fuess H and Madar R 2002 *Solid State Commun.* **124** 125
[16] Maignan A, Martin C, Hervieu M, Raveau B and Hejtmanek J 1998 *Solid State Commun.* **107** 363
[17] Damay F, Martin C, Maignan A and Raveau B 1997 *J. Appl. Phys.* **82** 6181